Precoder Design for Communication-Efficient Distributed MIMO Receivers with Controlled Peak-Average Power Ratio

Vinay A. Vaishampayan, *Fellow, IEEE,*

Abstract

We consider the problem of communicating over a relay-assisted multiple-input multiple-output (MIMO) channel with additive noise, in which physically separated relays forward quantized information to a central decoder where the transmitted message is to be decoded. We assume that channel state information is available in the transmitter and show that the design of a rational-forcing precoder—a precoder which is matched to the quantizers used in the relays—is beneficial for reducing the symbol error probability. It turns out that for such rational-forcing precoder based systems, there is natural tradeoff between the peak to average power ratio in the transmitter and the rate of communication between the relays and the central decoder. The precoder design problem is formulated mathematically, and several algorithms are developed for realizing this tradeoff. Optimality of the decoder communication rate is shown based on a result in distributed function computation. Numerical and simulation results show that a useful tradeoff can be obtained between the excess decoder communication rate and the peak-average power ratio in the transmitter.

***Index terms*—MIMO communication, peak to average power ratio, precoder, distributed function computation, lattices, lattice basis reduction, LLL algorithm, closest lattice point, decision feedback equalization, successive interference cancellation.**

I. Introduction

We consider a point-to-point, multiple-input multiple-output (MIMO), relay assisted communication problem in which spatially distributed relays are deployed between the transmitter and

V. A. Vaishampayan is with the Department of Engineering and Environmental Science, College of Staten Island, City University of New York, NY 10314, USA. e-mail: (see http://vinayvaishampayan.net.

the receiver. Each relay node (RN) forwards quantized information to a central receiver node (CN) over a noiseless link. The message is decoded by the CN. The combination of RNs and the CN will be referred to as the receiver. The communication system is illustrated in Fig. 1.

Mathematically, the communication problem is modeled by

$$\begin{aligned} \mathbf{x} &= \mathbf{H}\mathbf{y} + \mathbf{z} \\ \hat{x}_i &= q_i(x_i),\ i = 1, 2, \ldots, n, \\ \hat{\mathbf{y}} &= f(\hat{\mathbf{x}}), \end{aligned} \tag{1}$$

where $\mathbf{H} \in \mathbb{C}^{n\times n}$ is the channel response matrix, x_i, the i-th component of $\mathbf{x} \in \mathbb{C}^n$ is the observation at the i-th RN, $\mathbf{y}, \mathbf{z} \in \mathbb{C}^n$ represent the channel input and noise, respectively, $q_i : \mathbb{C}^n \to \mathbb{C}^n$ and $\hat{x}_i \in \mathbb{C}^n$ represent the quantizer mapping and output, respectively, and $f : \mathbb{C}^n \to \mathbb{C}^n$, $\hat{\mathbf{y}}$ represent the receiver mapping and output respectively. The channel input, or equivalently, modulator output $\mathbf{y}$ is assumed to take values in a modulation signal set with a finite number of modulation signals. $\mathbf{H}$ is assumed known precisely at the transmitter. The noise vector $\mathbf{z}$ is assumed to be independent of $\mathbf{y}$. We emphasize that the CN estimates $\mathbf{y}$ based on $\hat{\mathbf{x}}$, the quantized RN observations.

There are two distinct communication rates associated with this system, (i) the payload data rate, which is determined by the size of the modulation signal set, and (ii) the RN to CN communication rate, referred to as the decoder communication rate, which is determined by the quantizers deployed in each RN, in particular by the step size of a quantizer, if the quantizer is uniform. From information theoretic arguments, the decoder communication rate must exceed the payload data rate, in order to decode correctly. One of the objectives of this paper is to ensure that the difference between the decoder and payload rate is small. In this paper this difference is referred to as the *excess decoder communication rate* and is defined more precisely in Sec. IV-B.

A potential application of the above model is to relay backhaul enhancement systems which have been studied for improving cell-edge performance on the downlink in cellular systems, [28], [24], and are expected to be useful in rural and urban areas [28]. The link between the base-station (BS) and relay is referred to as the backhaul link, while the link between the relay and the

end-user is referred to as the access link. The objective of the relay is to enhance the end-to-end link quality. Here we assume that multiple relays serve a single end-user and that the access links are noiseless and orthogonal to one another and to the backhaul links. The setup is illustrated in Fig. 2.

Decoding complexity is a major problem in high data rate systems since, in general, joint decoding based on the entire $\hat{\mathbf{x}}$ is required in the CN. In order to manage the decoding complexity, several equalization strategies have been proposed and adopted in practice, most notably the VBLAST strategy which applies equalization in the receiver [12], [31]. In cases where the channel is known at the transmitter, the equalization strategy may take the form of a linear *precoder* [8], [29], [16]. A linear precoder $\mathbf{S} \in \mathbb{C}^{n\times n}$, maps an information vector $\mathbf{b} \in \mathbb{C}^n$ to the modulated signal $\mathbf{y}$ according to $\mathbf{y} = \mathbf{S}\mathbf{b}$ in such a way that $\mathbf{C} = \mathbf{H}\mathbf{S}$ is a lower triangular matrix with ones on the main diagonal. With such a precoding matrix, the channel output is given by

$$\mathbf{x} = \mathbf{C}\mathbf{b} + \mathbf{z}. \tag{2}$$

Consider for now, the situation where the CN has direct access to the RN inputs. Since

$$x_i = b_i + \sum_{j=1}^{i-1} c_{i,j} b_j + z_j, \;\; j = 1, 2, \ldots, n, \tag{3}$$

decoding of b_i can proceed sequentially in the order $i = 1, 2, \ldots, n$, dramatically reducing the decoding complexity, but with a loss in coding gain. This approach to equalization and decoding is known as decision feedback equalization (DFE). Here, as in prior works [8], [6], we will assume that $b_i \in \mathbb{Z}[\iota]$, where $\mathbb{Z}[\iota]$ is the set of complex integers, i.e. complex numbers with integer-valued real and imaginary parts ($\iota = \sqrt{-1}$).

In this work, the CN has access only to quantized observations of the RNs. We show that knowledge of the quantizers q_i can be exploited to design better precoders $\mathbf{S}$ (and thus $\mathbf{C}$), and we construct design algorithms, and quantify the improvements that can be obtained.

On a more theoretical level this work studies a natural consequence of applying in a MIMO system, a recently developed communication efficient method for decoding a lattice code, [3], [4], and shows that it leads to an interesting tradeoff between communication complexity and peak-

average power ratio (PAPR). Such communication efficient methods have their origins in *distributed function computation* (DFC) problems [30], [22]. We emphasize that communication complexity is well-studied in the DFC literature, but PAPR is purely a wireless concept.

A comprehensive discussion of strategies for reliable communication for the MIMO channel can be found in [29], [16]. Methods that apply a unitary transformation in the transmitter and DFE in the receiver are in [5], [21], [19], [29]. Most relevant to our work is a method proposed in [29], which uses decoder communication efficiently. We note that application of a unitary transformation in the modulator increases the PAPR, a fact that is also well known in OFDM systems [23], [17], [2], [7], [8]. In order to reduce the PAPR, methods that apply a unitary transformation in the decoder are proposed in [8], [29]. We note that Tomlinson-Harashima-Miyakawa (THM) precoding [27], [14], though invented in a different context (for inter-symbol interference channels), plays an essential role in these strategies, and will continue to do so in our work. Methods for improving the error probability in DFE receivers, through better basis selection are in [31], [6] and [10], where lattice reduction methods are shown to result in diversity gains on a fading channel.

A. Contributions of this Work

Our main contributions in this work are the following:

1) We show, through an error probability analysis, that *rational-forcing precoders* i.e. precoders designed such that the receive lattice generator matrix has rational entries, *matched* to the quantizer step sizes used by the RNs, are useful for achieving low error probability at a small decoder communication rate.
2) We show that a rational-forcing precoder leads in a natural way to a tradeoff between the RN-CN communication rate and PAPR in the transmitter.
3) Algorithms for computing rational-forcing precoder matrices are presented and achievable performance is presented through numerical calculations.
4) We show the information theoretic optimality of our proposed decoder communication strategy based on a known lower bound from the distributed function computation literature.
5) We show that receive lattice generators which are unimodular result in zero excess com-

munication cost. Identity matrices lie in this class, but the surprise here is that unimodular non-diagonal matrices lead to strict improvements in performance over identity matrices.

II. Outline of the Paper

Mathematical notation, definitions and some background material is in Sec. III. The system that we will work with is presented in Sec. IV. Quantization methods adopted in the RN's are described and expressions describing their impact on the error probability are developed in Sec. IV-A. Also, the excess decoder communication rate is defined. These calculations point to the useful nature of rational-forcing precoders (defined in Sec. IV-C) designed to achieve specific structured forms for the receive lattice. Algorithms for constructing precoders that trade excess decoder communication rate for PAPR are in Sec. V. Numerical computations and simulations are in Sec. VI, and the paper is summarized and conclusions are drawn in Sec. VII. A general result about the impact of quantization noise on the error probability is in App. B. Information theoretic optimality of the method of quantization described in Sec. IV-A is shown in App. C. Some specific matrices, included for repeatability purposes are in App. D.

III. Mathematical Notation and Preliminaries

For the mathematical development that follows we will use the following notation. For $x \in \mathbb{R}$, let $\lfloor x \rfloor$ to denote the greatest integer less than or equal to x (also referred to as rounding down), and $[x]$ to denote the nearest integer to x. Specifically, $[x] = \lfloor x + 1/2 \rfloor$. Thus $[1.5] = 2$ and $[-1.5] = -1$ or, equivalently, if $[x] = m$, then $m - 1/2 \leq x < m + 1/2$. The fractional part of $z \in \mathbb{R}$ is defined by $\{z\} = z - [z]$, $-1/2 \leq \{z\} < 1/2$. $\sqrt{-1}$ will be denoted by ι. If x is complex-valued, then $\lfloor x \rfloor$, $[x]$ and $\{x\}$ apply the corresponding operation independently to the real and imaginary parts. The set of complex integers, i.e. complex numbers whose real and imaginary parts are in $\mathbb{Z}$ is denoted $\mathbb{Z}[\iota]$. Matrices (vectors) will be written in boldface uppercase (lowercase). Vectors $\mathbf{x} = (x_1, x_2, \ldots, x_n)$ are to be regarded as column vectors. Matrix $\mathbf{M}^\dagger$ denotes the transposed conjugate of matrix $\mathbf{M}$. A lower (upper) triangular square matrix with ones on the main diagonal will be referred to as a unit lower (upper) triangular matrix. A matrix with entries from $\mathbb{Z}[\iota]$ is referred to as an integer matrix. A rational matrix $\mathbf{M}$ is one for which $d\mathbf{M}$ is an integer matrix, for some finite $d \in \mathbb{Z}$. For a vector with i repeated entries such

as $(\underbrace{a,\ldots,a}_{i \text{ times}},b)$ we will write $(a^{(i)},b)$. $\|\mathbf{x}\|$ is the standard Euclidean norm. $\mathbf{A}(a:b,c:d)$ is the submatrix of $\mathbf{A}$ restricted to rows $a,a+1,\ldots,b$ and columns $c,c+1,\ldots,d$. Traditionally, realizations of random variables are denoted by a lower case version of the random variable. For notational simplicity, we will not make an explicit distinction between a random variable and its realization—this should be obvious from the context. The expected value of random variable x is denoted $E[x]$ and the probability of an event $\mathcal{A}$ is denoted *Prob*$(\mathcal{A})$. Suppose random variable $x=x_r+\iota x_i$ is such that $x_r,x_i\sim\mathcal{N}(0,\sigma^2)$ are independent, then we say that $x\sim\mathcal{N}(0,\sigma^2)$. The standard complementary error function is *erfc*$(x)=(2/\sqrt{\pi})\int_x^\infty e^{-t^2}dt$. By $a=b \pmod m$, for $a,b,m\in\mathbb{Z}$, we mean $a\in\{0,1,\ldots,m-1\}$ and $a-b$ is divisible by m. A rectangular subset of $\mathcal{C}^n$ is a set of the form $\{\mathbf{x}\in\mathcal{C}^n \ : \ a_i\le Re(x_i)\le b_i, c_i\le Im(x_i)\le d_i,\ i=1,2,\ldots,n\}$.

A. Peak-Average Ratio

For $n\times n$ complex-valued matrix $\mathbf{Q}$, let

$$||\mathbf{Q}||_\infty=\max_{1\le i\le n}\sum_{j=1}^{n}|q(i,j)| \tag{4}$$

denote its maximum row-sum matrix norm (also called the ∞-norm) [15]. Let $\mathbf{y}=\mathbf{Q}\mathbf{x}$. The peak-to-average power ratio (PAPR) is defined as [11], [7]

$$\gamma=\frac{\max_{1\le j\le n}|y_j|}{E[\|\mathbf{y}\|^2/n]^{1/2}}.$$

If $\mathbf{Q}$ is unitary and the real and imaginary parts of $\mathbf{x}$ are uniformly distributed on $[-A/2,A/2]^n$, then $E\|\mathbf{y}\|^2=E\|\mathbf{x}\|^2=nA^2/6$, and $\gamma=\sqrt{3/2}||\mathbf{Q}||_\infty$. Thus it will suffice to define the peak-average power ratio by

$$\gamma=||\mathbf{Q}||_\infty. \tag{5}$$

B. Lattices

A *lattice* $\Lambda\subset\mathbb{C}^n$ with generator matrix $\mathbf{C}\in\mathcal{C}^{n\times n}$, is the set $\{\mathbf{C}\mathbf{b},\ \mathbf{b}\in\mathbb{Z}[\iota]^n\}$. We will assume that $\mathbf{C}$ has full rank.

The objective of the *closest vector problem (CVP)* for a lattice is to solve

$$\hat{\mathbf{b}} = \underset{\mathbf{u}\in\mathbb{Z}[\iota]^n}{\arg\min} \mid\mid \mathbf{x} - \mathbf{C}\mathbf{u} \mid\mid^2 \tag{6}$$

for a given $\mathbf{x} \in \mathbb{C}^n$. Since the CVP is NP-hard, an approximate solution, referred to as the Babai point is often computed [1]. In the special case where $\mathbf{C}$ is a unit lower triangular matrix, the Babai point $\hat{\mathbf{b}}$ is obtained by solving[1]

$$\hat{b}_m = \left[x_m - \sum_{l=1}^{m-1} c_{m,l}\hat{b}_l \right], \tag{7}$$

in the order $m = 1, 2, \ldots, n$. For a MIMO communication system with channel $\mathbf{H}$, suppose a precoder $\mathbf{S}$ is chosen such that $\mathbf{HS} = \mathbf{C}$ is unit lower triangular. The maximum likelihood of estimate of $\mathbf{b}$ based on $\mathbf{x} = \mathbf{HSb} + \mathbf{z}$, where $\mathbf{z} \sim \mathcal{N}(0, \sigma^2)$, is given by (7). Thus DFE decoding is equivalent to computation of the Babai point.

Definition 1 (Receive Lattice)**.** *The lattice at the output of the channel, in the absence of channel noise, is called the Receive Lattice.*

Thus $\mathbf{HS}$ is a generator for the *receive lattice*, corresponding to precoder $\mathbf{S}$ and channel matrix $\mathbf{H}$ in (2).

IV. System Description

The system that we work with has already been described already in (1). From here on we will assume that the i-th component of the received vector $\mathbf{x}$ is quantized at the i-th RN with a *uniform threshold* quantizer and sent to the CN. The justification for using a uniform threshold quantizer will become clear when we analyze the error probability later in this section. The channel matrix $\mathbf{H}$ is known at the transmitter (full CSI). It is also assumed that b_i, the i-th component of the information vector $\mathbf{b}$ has real and imaginary parts in the set $\{0, 1, \ldots, a_i - 1\}$, for some integers a_i, $i = 1, 2, \ldots, n$. Thus $\mathbf{b}$ is restricted to a rectangular subset $\mathcal{B} \subset \mathbb{Z}[\iota]^n$.

Our objective is to construct a precoding matrix $\mathbf{S}$ such that (i) a DFE decoder can be implemented in the CN (for managing the decoder complexity) (ii) the transmit power is as

[1]Recall that $[x]$ is x rounded to the nearest integer.

small as possible, and, (iii) the error probability P_e is as small as possible, given that the CN has access to *quantized* information from the RN. We will see that our precoder setup has sufficient flexibility to allow us to satisfy one additional design constraint, namely, (iv) minimize the PAPR at the transmitter.

We address items (i)-(iii) and provide an explanation for item (iv) in the remainder of this section. The design issue raised in item (iv) is addressed in Sec. V, where we will see that a natural tradeoff exists between the amount of communication between the RNs and the CN and the PAPR.

We have already seen that in order to satisfy condition (i) $\mathbf{S}$ should be chosen such that the generator matrix of the receive lattice,

$$\mathbf{C} = \mathbf{HS} \tag{8}$$

is a unit lower triangular matrix.

With reference to condition (ii), we note that since $\mathbf{b}$ is assumed to be in a rectangular subset of $\mathbb{C}^n$, the set $\{\mathbf{Sb},\ \mathbf{b} \in \mathcal{B}\}$ will in general be a skewed and rotated parallelepided, which results in an increased transmit power. Thus, the linear map $\mathbf{S}$ should not be implemented directly. This situation is rectified by using a Tomlinson-Harashima-Miyakawa (THM) precoder [27], [14], which effectively computes a modified information vector $\mathbf{b}'$ based on $\mathbf{b}$. The mapping between $\mathbf{b}$ and $\mathbf{b}'$ is one-one and invertible. Let the QR factorization of $\mathbf{S}$ give $\mathbf{S} = \mathbf{QR}$, where $\mathbf{Q}$ is unitary and $\mathbf{R}$ is upper triangular with real entries on the main diagonal. Further, let $\mathbf{R} = \mathbf{MV}$, where $\mathbf{M}$ is a diagonal matrix with real entries and $\mathbf{V}$ is unit upper triangular. In terms of the modified information vector $\mathbf{b}'$, the transmitted vector $\mathbf{y}$ is given by

$$\mathbf{y} = \mathbf{QMVb}'. \tag{9}$$

The THM precoder ensures that $\mathbf{w} = \mathbf{MVb}'$ lies in a rectangular region, specifically, the real and imaginary parts of each component of $\mathbf{w}$ lie in the interval $[-A/2, A/2]$. Since $\mathbf{Q}$ is unitary and upon assuming that a uniform distribution for the real and imaginary parts of each w_i, the transmitted energy per signaling interval is $E[\|\mathbf{y}\|^2] = E[\|\mathbf{w}\|^2] = nA^2/12$. Note however, that the set $\mathbf{Qw}$ is a rotated hyper-rectangle, which leads to an increase in PAPR for non-trivial

$\mathbf{Q}$. This explains item (iv) above. Implementation details of the THM precoder are provided in App. A. The associated processing chain is illustrated in Fig. 3, where we use the notation $\boxed{\mathbf{V}}$ to denote a THM implementation of $\mathbf{V}$. Finally we note that the payload data rate per signaling interval is for large A well approximated by $n \log_2 A + \log_2 |\det \mathbf{H}|$.

Definition 2. *A precoder* $\mathbf{S}$ *for which* $\mathbf{C} = \mathbf{HS}$ *is a rational matrix is called a* **rational forcing precoder**.

In order to satisfy condition (iii), it is beneficial to match the precoder to the quantization in the RN, more specifically, to design $\mathbf{S}$ to be rational-forcing, such that the off-diagonal rational entries of $\mathbf{C}$ have denominators determined by the quantizer step size. This result is developed next, in Sec. IV-A. Optimality of the quantization method for a given rational $\mathbf{C}$, a dual result, is shown in App. C.

A. Quantization in the RN and its Impact on the Error Probability

From (1), (8) and (31), the received signal at the RNs is $\mathbf{x} = \mathbf{C}\mathbf{b}' + \mathbf{z}$ where $\mathbf{C}$ which is unit lower triangular by design. Thus

$$x_i = b'_i + \sum_{j=1}^{i-1} c_{i,j} b'_j + z_i, \quad i = 1, 2, \ldots, n. \tag{10}$$

In our setup, x_i, the observation at the ith RN, is quantized with a uniform quantizer. Entropy coded bin indices are then sent to the CN. In particular, we assume that the ith RN uses a quantizer step size $1/s_1 = 1$ and $1/s_i,\ i = 2, 3, \ldots, n$, where s_i an integer. The CN then estimates the data vector $\mathbf{b}$ based on $\hat{\mathbf{x}} = (\hat{x}_1, \hat{x}_2, \ldots, \hat{x}_n)$, where $\hat{x}_i$ is the quantized estimate of x_i available in the CN.

We now show that precoder design matched to the quantizer results in reduced symbol error probability. Towards this end we consider two cases: (i) $\mathbf{C}$ is a unit lower triangular matrix, (ii) $\mathbf{C}$ is a rational unit lower triangular matrix with entries matched to the quantizer step sizes $1/s_i$. Assume that the CN starts decoding b'_i in the order $i = 1, 2, \ldots, n$. We calculate the conditional error probability

$$\textit{Prob}\left(\hat{b}'_i = b'_i | \hat{b'}_j = b'_j,\ j = 1, 2, \ldots, i-1\right)$$

in the above two cases. Let ν_i be the quantized value sent from the ith RN to the CN and let $t = \sum_{j=1}^{i-1} c_{i,j} b'_j$ be the interference. For the purposes of the analysis that follows it suffices to work with the real or the imaginary parts of ν_i and t. In order to keep the notation simple, we will assume that ν_i and t are real and that the noise variable $z_i \sim \mathcal{N}(0, \sigma^2)$ is real-valued as well.

(i) Let the ith RN send $\nu_i = [sx_i]$ to the CN. Let $t = \sum_{j=1}^{i-1} c_{i,j} b'_j$. Then given previous correctly recovered data, the maximum-likelihood estimate of b'_i at the CN is obtained by rounding

$$\begin{aligned} \frac{\nu_i - st}{s} &= \frac{[s(b'_i + t + z_i)] - st}{s} \\ &= b'_i + \frac{[s(t + z_i)] - st}{s} \\ &= b'_i + \frac{1}{s}\left([s(t + z_i)] - s(t + z_i)\right) + z_i \\ &= b'_i + z_i - \frac{\{s(t + z_i)\}}{s}. \end{aligned} \tag{11}$$

Note that the interference t is present in the noise term in the above equation. Since $\{s(t+z_i)\}/s$ is to a good approximation independent of z_i and uniformly distributed on $[-1/2, 1/2)$, it follows by conditioning on the on the event $\{s(t + z_i)\}/s = \alpha$ that the error probability in recovering b'_i is given by

$$\int_{1/2}^{1/2} \left(F_{z_i}\left(\frac{1}{2} - \frac{\alpha}{s}\right) - F_{z_i}\left(-\frac{1}{2} - \frac{\alpha}{s}\right)\right) d\alpha. \tag{12}$$

When $z_i \sim \mathcal{N}(0, \sigma^2)$, the error probability is upper bounded by

$$\textit{Prob}\left(|Re(z_i)| < \left(\frac{1}{2} - \frac{1}{2s}\right)\right) = \text{erfc}\left(\frac{s-1}{2s\sqrt{2}\sigma}\right). \tag{13}$$

The upper bound becomes tighter as s becomes larger.

(ii) Once again let $t = \sum_{j=1}^{i-1} c_{i,j} b'_j$. However, since the entries in $\mathbf{C}$ are rational, $t = r/s$ for integer r, s, which are relatively prime to one another. If s is odd, the RN sends $\nu_i = [sx_i]$ to the CN. If s is even the RN sends $\nu_i = \lfloor sx_i \rfloor$ to the CN. Thus by repeating the steps in (11), the ML estimate of b'_i is now obtained by rounding

$$\frac{\nu_i - st}{s} = b'_i + \frac{[sz_i]}{s}. \tag{14}$$

Notice the absence of the interference term in the noise when comparing (14) and (11). The error probability is given by

$$\textit{Prob}(|z_i| < 1/2) = \text{erfc}\left(\frac{1}{2\sqrt{2}\sigma}\right). \tag{15}$$

Fig. 4, described in detail in Sec. VI, shows that for small s, (12) is significantly larger than (15).

Remark 1. *The above analysis shows that rational-forcing-precoders have an advantage over precoders that do not enforce such a constraint, and lead to an interference-free noise term as can be seen by comparing* (14) *and* (11)*.*

A result which shows that the error probability is not limited by the quantization noise, provided the quantizer is suitably fine, is proved in App. B. This result is more general, but less quantitative as compared to (13). Optimality of the quantization method described here is proved in App. C.

B. Excess Decoder Rate Definition

We now define the excess decoder communication rate when the i-th RN uses a uniform quantizer with step size $1/s_i$, $i = 2, \ldots, n$. We assume that $s_1 = 1$. In order to do so we choose as a baseline system, a hypothetical system where x_i is known precisely in the CN. In this system a DFE would estimate b'_i by rounding to the nearest integer, i.e. the estimate obtained would be given by

$$\hat{b}'_i = \left\lceil x_i - \sum_{j=1}^{i-1} c_{i,j}\hat{b'}_j \right\rfloor, \ i = 1, \ldots, n. \tag{16}$$

Note that the baseline system effectively applies a quantizer with a step size of unity. We will consider this to be our baseline step size.

Definition 3. *The excess decoder communication rate when the i-th RN uses a uniform quantizer with step size $1/s_i$, $i = 2, 3, \ldots, n$ is defined as*

$$R_{dec,ex} = \frac{1}{n}\sum_{i=2}^{n} \log_2 s_i \ \textit{bits/signaling interval/RN}. \tag{17}$$

C. Receive Lattice Generators with Small Communication Requirements

Definition 4. *Given positive integers $d_2, \ldots, d_n$, let $\mathcal{C}(d_2, \ldots, d_n)$ be the set of unit lower triangular rational matrices in which all entries in row i, real and imaginary, except on the main diagonal, can be expressed as a rationals with denominator d_i, $i = 2, 3, \ldots, n$.*

If a precoder is designed such that $\mathbf{C} \in \mathcal{C}(d_2, \ldots, d_n)$, and if we set $s_1 = 1$ and $s_i = d_i$, $i = 2, \ldots, n$, where the quantizer step size in the i-th RN is $1/s_i$, it follows from (15) that interference free decoding is achieved. For clarity we show a few examples along with their excess communication rates when the quantizer and precoder are matched.

Example 1.

$$\mathbf{C}_0 = \mathbf{I}, \quad \mathbf{C_1} = \begin{pmatrix} 1 & 0 & 0 & 0 \\ -1 & 1 & 0 & 0 \\ 0 & -1 & 1 & 0 \\ 1 & 2 & 3 & 1 \end{pmatrix}.$$

These are examples of unimodular matrices, since all entries are integer valued and all have absolute value of determinant equal to unity. The excess decoder communication rate, $R_{dec,ex}$, for all unit-triangular, unimodular matrices is 0 bits.

Example 2.

$$\mathbf{C} = \begin{pmatrix} 1 & 0 & 0 & 0 \\ 1/2 & 1 & 0 & 0 \\ 1/4 & 1/3 & 1 & 0 \\ 1/8 & 1/4 & 1/3 & 1 \end{pmatrix}.$$

The excess communication rate is 0 for the first row, 1 bit for the second row, $\lceil \log_2(12) \rceil = 4$ bits for the 3rd row and $\lceil \log_2(24) \rceil = 5$ bits for the last row. The average decoder excess communication rate, $R_{dec,ex}$ is 2.5 bits.

From these examples it should be clear that if all the off-diagonal entries in the ith row of

a rational unit lower triangular generator matrix can be written with a common denominator of $d_i > 0$, $i = 2, 3, \ldots, n$, then the excess decoder communication rate is upper bounded by $\sum_{i=2}^{n} \lceil \log_2 d_i \rceil$.

As mentioned earlier, we prove a complementary result in App. C, where we show that if $\mathbf{C} \in \mathcal{C}(d_2, \ldots, d_n)$, the optimal quantizer is a uniform quantizer.

V. Precoder Design Algorithms for PAPR Control

As we have seen, implementation of our precoder involves the application of a unitary matrix $\mathbf{Q}$. As it turns out, we have some flexibility in choosing $\mathbf{S}$ to minimize $||\mathbf{Q}||_\infty$. Our objective now is to construct a precoder matrix $\mathbf{S}$ such that the receive lattice generator $\mathbf{C} \in \mathcal{C}(d_2, \ldots, d_n)$ and such that the QR factorization of $\mathbf{S}$ results in $\mathbf{Q}$ with small $||\mathbf{Q}||_\infty$. We will assume that $\mathbf{H}$ is invertible, has an LU factorization, and that the rows of $\mathbf{H}$ have been rearranged if necessary, using the partial pivot strategy described in [13]. Let $\mathbf{G} = \mathbf{H}^{-1}$. Our 'wishful' objective is as follows.

Objective 1. *Find* $\mathbf{C} \in \mathcal{C}(d_2, \ldots, d_n)$ *such that* $||\mathbf{Q}||_\infty$ *is minimized, where* $\mathbf{Q}$ *is the unitary matrix obtained from the QR factorization of* $\mathbf{S} = \mathbf{GC}$.

Unfortunately, the problem appears to be intractable. A more tractable objective is presented next. We explain the intuition behind this approach first. Consider the factorization $\mathbf{S} = \mathbf{QR}$, where $\mathbf{Q}$ is a unitary matrix and $\mathbf{R}$ is upper triangular. If $\mathbf{S}$ is upper triangular then, $\mathbf{Q} = \mathbf{I}$, the identity matrix, which has small $||\mathbf{Q}||_\infty$. Thus it may be worthwhile searching for $\mathbf{C}$ such that $\mathbf{S}$ is approximately upper triangular. Remember however, that we are restricted in our selection of $\mathbf{C}$, but that the constraints imposed by $\mathcal{C}(d_2, \ldots, d_n)$ become less stringent as we allow $d_1, \ldots, d_n$ to become larger. Additional motivation comes from the continuity result [25], Thm. 3.1, which establishes a bound on the norm of the perturbation of $\mathbf{Q}$ in terms of a perturbation of $\mathbf{S}$, in terms of the condition number of $\mathbf{S}$. With the intuition explained, we now present our, more tractable, objective.

Objective 2. *Find* $\mathbf{C} \in \mathcal{C}(d_2, \ldots, d_n)$ *such* $\mathbf{S} = \mathbf{GC}$ *is approximately upper triangular.*

The sense of approximation will become clearer in the algorithms that are described later.

Algorithms for obtaining $\mathbf{C}$ and the associated precoder $\mathbf{S}$ are now presented. Let the LU factorization of the channel matrix $\mathbf{H}$, result in $\mathbf{H} = \mathbf{L}\mathbf{V}^{-1}$, where $\mathbf{L}$ is unit lower triangular, $\mathbf{V}^{-1}$ is upper triangular.

A. Algorithm A1: Direct Quantization

The first algorithm sets $\mathbf{C}$ to a quantized version of $\mathbf{L}$.

Algorithm 1.

1) *Compute the LU factorization* $\mathbf{H} = \mathbf{L}\mathbf{V}^{-1}$, $\mathbf{L}$ *unit lower triangular.*
2) *Determine* $\mathbf{C}$ *by setting* $c_{i,j} = \lfloor l_{i,j} d_i + 1/2 \rfloor / d_i$, $1 \leq j < i \leq n$.
3) *Apply the QR factorization to* $\mathbf{S} = \mathbf{H}^{-1}\mathbf{C}$ *to get* $\mathbf{S} = \mathbf{Q}\mathbf{R}$.

B. Algorithm A2: Nearest Lattice Point Algorithm

We start with a less formal description and illustrative example before providing a formal description of the second algorithm. Our objective is determine $\mathbf{C} \in \mathcal{C}(d_2, \ldots, d_n)$ so that $\mathbf{S} = \mathbf{G}\mathbf{C}$ is approximately upper triangular.

Consider the computation of $\mathbf{c}_i$, the ith column of $\mathbf{C}$, which is of the form

$$\mathbf{c}_i = (0^{i-1}, 1, m_{i+1,i}/d_{i+1}, m_{i+2,i}/d_{i+2}, \ldots, m_{n,i}/d_n),$$

where the $m_{i,j}$'s are in $\mathbb{Z}[\iota]$ and the d_i's are positive integers. Our objective is to find $\mathbf{c}_i$ such that $\mathbf{G}\mathbf{c}_i$ approximates

$$\begin{pmatrix} *^i \\ 0^{n-i} \end{pmatrix} \tag{18}$$

where the first i entries marked $*$ are arbitrary. The last $n-i+1$ entries of $\mathbf{c}_i$ (positions $i, \ldots, n$) can be written as

$$\underbrace{\begin{pmatrix} 1 & & & \\ & \frac{1}{d_{i+1}} & & \\ & & \ddots & \\ & & & \frac{1}{d_n} \end{pmatrix}}_{\mathbf{D}} \underbrace{\begin{pmatrix} 1 \\ m_{i+1,i} \\ \vdots \\ m_{n,i} \end{pmatrix}}_{\tilde{\mathbf{m}}}. \tag{19}$$

Let

$$\tilde{\mathbf{G}} = \mathbf{G}(i+1:n, i:n)\mathbf{D} = \begin{pmatrix} \mathbf{t} & \mathbf{A} \end{pmatrix} \tag{20}$$

where the first column $\mathbf{t}$ is a vector of size $n-i$ and $\mathbf{A}$ is of size $(n-i)\times(n-i)$. Let $\tilde{\mathbf{m}} = (1, \mathbf{m})$. Our objective is to solve the equation

$$\mathbf{t} + \mathbf{A}\mathbf{m} = \mathbf{0}. \tag{21}$$

approximately (an exact solution is not possible in general because $\mathbf{m} \in \mathbb{Z}[\iota]^n$). This can be accomplished by solving

$$\mathbf{m} = \arg \min_{\mathbf{q}\in\mathbb{Z}[\iota]^{n-i}} \|\mathbf{t} + \mathbf{A}\mathbf{q}\|. \tag{22}$$

Example 3. *Let*

$$\mathbf{G} = \begin{pmatrix} -0.1250 & 1.4929 & .6129 \\ 0.8381 & -1.5975 & -1.3468 \\ 0.1604 & -0.2305 & -0.9240 \end{pmatrix}$$

Obtain $\mathbf{C} \in \mathcal{C}(2, 8)$.

Solution 1. *First consider* $\mathbf{c}_1 = (1, m_{2,1}/2, m_{3,1}/8)$*, the first column of* $\mathbf{C}$*. We obtain*

$$\tilde{\mathbf{G}} = \begin{pmatrix} 0.8381 & -0.7987 & -0.1683 \\ 0.1604 & -0.1153 & -0.1155 \end{pmatrix}. \tag{23}$$

and search for $(m_{2,1}, m_{3,1})$ *to minimize*

$$\left\| \begin{pmatrix} 0.8381 \\ 0.1604 \end{pmatrix} + \begin{pmatrix} -0.7987 & -0.1683 \\ -0.1153 & -0.1155 \end{pmatrix} \begin{pmatrix} m_{2,1} \\ m_{3,1} \end{pmatrix} \right\|, \tag{24}$$

whose solution is $(m_{2,1}, m_{3,1}) = (1, 0)$*. Similarly for the second column* $\mathbf{c}_2 = (0, 1, m_{3,2}/8)$*, we minimize*

$$\| - 0.1153 - 0.1155 m_{3,2} \| \tag{25}$$

to get $m_{3,2} = -2$ *and thus* $\mathbf{C} = \begin{pmatrix} 1 & 0 & 0 \\ 1/2 & 1 & 0 \\ 0 & -2/8 & 1 \end{pmatrix}$. *Since every element in the last row of* $\mathbf{C}$ *can be written with denominator* 4*, the excess communication rate,* $R_{dec,ex}$ *is* $(1+2)/3 = 1$ *bit/RN which is smaller than the typical excess cost for* $\mathcal{C}(2,8)$ *which is* $4/3$ *bits/RN.*

Algorithm 2.

1) `for` $i = 1$ *to* $n-1$ `do`
2) *Construct* $\tilde{\mathbf{G}}$*,* $\mathbf{T}$ *and* $\mathbf{A}$ *as in* (20)*.*
3) *Determine* $\mathbf{m}$ *by solving* (22)*.*
4) *Set* $c_{i+j,i} = m_{j,i}/d_j$*,* $j = 1, \ldots, n-i$*.*
5) `end for`
6) $\mathbf{S} = \mathbf{GC}$
7) *Calculate QR factorization* $\mathbf{S} = \mathbf{QR}$*.*

Note that in the limit as the d_i's become large, $\mathbf{C}$ converges to the unit lower triangular matrix $\mathbf{L}$ obtained by the LU factorization $\mathbf{H} = \mathbf{L}\mathbf{V}^{-1}$. Thus $\mathbf{S}$ converges to $\mathbf{H}^{-1}\mathbf{L} = \mathbf{V}$, which is upper triangular, $\mathbf{Q}$ in the QR factorization of $\mathbf{S}$ converges to the identity matrix and $\mathbf{R}$ converges to $\mathbf{V}$. On the other hand, when $d_i = 1$, $i = 2, \ldots, n$, $\mathbf{C}$ is a unit lower triangular matrix with integer entries—thus it is unimodular. Note that $\mathbf{I}$, the identity matrix lies in this class, but the formulation allows for the possibility of other unimodular matrices to achieve zero excess communication cost.

C. On LLL-reducedness of $\mathbf{C}$

Finally, we comment about quality—in terms of LLL-reducedness [18]— of the receive lattice generator matrices $\mathbf{C} \in \mathcal{C}(d_2, \ldots, d_n)$. It is now well-known [31], [10], [6] that the probability that the SIC solution coincides with the true ILS solution is larger when $\mathbf{C}$ is LLL-reduced. For a unit lower triangular matrix, $\mathbf{C}$, since the Gram-Schmidt orthogonalization process starting from the last column results in the orthogonal matrix which is the identity matrix, the well-known conditions for being LLL-reduced reduce to

1) $|c_{i,j}| \leq 1/2$, $1 \leq j < i \leq n$
2) $1 + c_{i+1,i}^2 \geq 3/4$

Consider $\mathcal{C}(d_2, \ldots, d_n)$, for $d_i > 0$, $i = 2, \ldots, n$. The second condition is always satisfied for any matrix in $\mathcal{C}(d_2, \ldots, d_n)$ and it is possible, using only elementary integer linear column operations, to reduce any matrix in this set to another matrix in the same set which satisfies the first condition, without destroying the second property. In fact, $\mathbf{C}$ can be LLL-reduced by multiplication on the right with a lower triangular unimodular matrix. This LLL-reduced matrix may then be used for decoding, without affecting the communication cost. Hence, even though the algorithms presented are not guaranteed to find $\mathbf{C}$ which is LLL-reduced, an equivalent LLL-reduced matrix can be found quite easily.

Another interesting observation is when $d_i = 1$, $i = 2, \ldots, n$, any matrix in $\mathcal{C}(d_2, \ldots, d_n)$ is unimodular. Thus *any two* matrices in $\mathbf{C}_1, \mathbf{C}_2 \in \mathcal{C}(1^{(n-1)})$ are related by $\mathbf{C}_1 = \mathbf{C}_2\Delta$, where Δ is unimodular lower triangular. Since the identity matrix $\mathbf{I} \in \mathcal{C}(1^{(n-1)})$, the processing chain can be simplified from $\mathbf{C}^{-1}\mathbf{HQM}\boxed{\mathbf{V}}$ to $\mathbf{HQM}\boxed{\mathbf{V}}$, and this solution requires no decoder cooperation. However, as we will see in Sec. VI, significant PAPR gains are obtained.

D. Algorithm A3: Block Reduction

Our last approach for managing $||\mathbf{Q}||_\infty$, is to construct $\mathbf{C}$ in such a way that $\mathbf{Q}$ is approximately block-diagonal. We consider such structured approaches here. We begin with an example.

Suppose $n = 7$. Partition $\mathbf{C}$ as follows

$$\mathbf{C} = \begin{pmatrix} \mathbf{C}_{11} & \mathbf{0} & \mathbf{0} \\ \mathbf{C}_{21} & \mathbf{C}_{22} & \mathbf{0} \\ \mathbf{C}_{31} & \mathbf{C}_{32} & \mathbf{C}_{33} \end{pmatrix}.$$

Here $\mathbf{C}_{ii}$ are unit lower triangular square matrices of size 2, 3 and 2, for $i = 1, 2, 3$, respectively. The upper triangular blocks have been set to zero, $\mathbf{C}_{ij} = \mathbf{0}$ for $j > i$, so the matrix is block-unit-lower triangular. The size of the remaining blocks is thus fully determined. Let $\mathbf{S} = \mathbf{GC}$. Our objective is to choose $\mathbf{C}$ in such a way that the QR factorization $\mathbf{S} = \mathbf{QR}$ results in block

diagonal

$$\mathbf{Q} = \begin{pmatrix} \mathbf{Q}_1 & & \\ & \mathbf{Q}_2 & \\ & & \mathbf{Q}_3 \end{pmatrix} \tag{26}$$

in a limiting sense to be made more precise, where $\mathbf{Q}_i,\ i = 1, 2, 3$ are of size 2, 3 and 2, resp. The idea is to limit $||\mathbf{Q}||_\infty$ by limiting the support of each row of $\mathbf{Q}$.

This, too, can be accomplished through a nearest lattice point search. In more detail, suppose $\mathbf{C}_{ii}$, $i = 1, 2, 3$ are some fixed unimodular unit lower triangular matrices. Then individual columns of the submatrix

$$\begin{pmatrix} \mathbf{C}_{21} \\ \mathbf{C}_{31} \end{pmatrix}$$

can be obtained by minimizing

$$\left\| \begin{pmatrix} \mathbf{G}_{21} \\ \mathbf{G}_{22} \end{pmatrix} \mathbf{C}_{11} + \begin{pmatrix} \mathbf{G}_{22} & \mathbf{G}_{23} \\ \mathbf{G}_{32} & \mathbf{G}_{33} \end{pmatrix} \begin{pmatrix} \mathbf{C}_{21} \\ \mathbf{C}_{31} \end{pmatrix} \right\| \tag{27}$$

columnwise through a lattice point search. Similarly the columns of $\mathbf{C}_{32}$ can be obtained by minimizing

$$\|\mathbf{G}_{32}\mathbf{C}_{22} + \mathbf{G}_{33}\mathbf{C}_{32}\| \tag{28}$$

columnwise through a lattice point search. Clearly many possibilities exist for partitioning the matrices. We do not state a formal algorithm because the steps should be obvious given the description of Algorithm 2.

VI. Numerical Experiments

We now describe two systems for purposes of comparison, as well as the system proposed in this work, after which experimental results are discussed.

A. Systems for Comparison

Strategy S1: Let $\mathbf{H}^{-1} = \mathbf{QR}$, where $\mathbf{Q}$ is a unitary matrix and $\mathbf{R}$ is triangular. Let $\mathbf{R} = \mathbf{MU}^{-1}$, where $\mathbf{M}$ is a diagonal matrix and $\mathbf{U}$ is unit trangular. Thus the receive lattice has

generator matrix $\mathbf{U} = \mathbf{HQM}$. The encoder precodes the data using the precoder matrix $\mathbf{S} = \mathbf{QM}$ and the transmitted vector is $\mathbf{y} = \mathbf{QMb}$, where the i-th component of $\mathbf{b}$ (both the real and imaginary parts) can assume $2\lfloor A/(2m_i)\rfloor + 1$ distinct values, where m_i is the absolute value of the i-th diagonal entry of $\mathbf{M}$ and A is an integer chosen to control the payload data rate. The observation of the ith RN is quantized using stepsize $1/d_i$, and $d_1 = 1$. The decoder in the CN is a DFE for the receive lattice $\mathbf{U}$, which operates on quantized values received from each RN. Note that for large A, the payload data rate is approximately given by $n\log_2(A) + \log_2|\det \mathbf{H}|$ and the transmit energy per signaling interval is approximately given by $nA^2/12$. However, unlike with the rational-forcing precoder, the resulting receive lattice generator $\mathbf{U}$ need not have rational entries. Note that the measured PAPR for the matrix $\mathbf{Q}$ based on the channel matrix $\mathbf{H} = \mathbf{H}_1$, shown in App. D is 1.98 (we set this to 0 dB for this example).

Strategy S2: Same factorization of $\mathbf{H}$ as above. However, transmitter processing chain applies $\mathbf{R}$ (this requires the use of THM precoding which we describe later) in the transmitter, followed by $\mathbf{Q}$. Since $\mathbf{HQR} = \mathbf{I}$, the receive lattice generator is the identity matrix. Thus the demodulator sees n independent channels, and the excess communication cost is zero. DFE detection factors into n independent detectors. The transmit power and payload data rate is the same as for Strategy S1. While this strategy was proposed for a broadcast scenario in [29] and improved in [10], it applies very well to the situation considered in this work. The PAPR is identical to the previous case, thus 0 dB.

Strategy S3: This is the system proposed in this work, which is based on a rational forcing precoder $\mathbf{S}$, and results in the receive lattice generator matrix $\mathbf{C} = \mathbf{HS}$. Generator matrix $\mathbf{C}$ has been matched to the quantizer step sizes used by the RNs. Specifically if the quantizers step sizes are $1/s_1 = 1$, and $1/s_i$, $i = 2, \ldots, n$, s_i integer, then $\mathbf{C}$ is in $\mathcal{C}(d_2, d_3, \ldots, d_n)$, where $d_i = s_i,\ i = 2, 3, \ldots, n$. The factorization $\mathbf{S} = \mathbf{QMV}$ as in (9) yields the encoder processing chain $\mathbf{QM}\boxed{\mathbf{V}}$. The i-th component of the information vector (real and imaginary parts) is chosen to lie in the set $\{0, 1, \ldots, a_i - 1\}$, where $a_i = 2\lfloor A/(2m_i) - 1/2\rfloor + 1$, where m_i is the absolute value of the i-th diagonal entry of $\mathbf{M}$ and A is an integer chosen to control the payload data rate. Note that for large A, the payload data rate is approximately given by $n\log_2(A) + \log_2|\det \mathbf{H}|$ and the transmit energy per signaling interval is approximately given by $nA^2/12$. With $\mathbf{H} = \mathbf{H}_1$

and $\mathbf{C} = \mathbf{C}_1$, where $\mathbf{H}_1, \mathbf{C}_1$ are shown in App. D, interestingly, even at zero cooperation cost, a PAPR of 1.49 is obtained for this example, which is smaller than that achieved by S2 and S1 by 2.4 dB. Further, S3 is able to trade communication cost for PAPR.

B. Numerical Results

Fig. 4, compares the error probability in recovering $\mathbf{b}$ obtained by (12) for a precoder in which the receive lattice is a unit triangular matrix with complex entries, to the error probability obtained using (15), which is for a rational-forcing precoder. Results are presented for quantizer step sizes of 2^{-i}, $i = 1, 2, 3, 4$, where i is the excess communication rate identified in the figure. This figure equivalently displays the error probability for Strategies S1, S2 and S3, described in Sec. I-A, since only S2 and S3 are based on rational-forcing precoders.

We implemented Algorithms A1-A3, in order to find $\mathbf{C}, \mathbf{S}$. We then implemented the distributed rational-forcing precoder system of Fig. 3 in software. For the nearest lattice point search we used the MATLAB implementation of the LLL algorithm [20]. Fig. 5 shows the tradeoff between the excess communication rate $R_{dec,ex}$ and the relative PAPR, obtained for two randomly selected channel matrices $\mathbf{H}_6$ and $\mathbf{H}_6(block)$, which are shown in App. D, with $n = 6$. The relative PAPR is defined to be $20 * log_{10}(\gamma/\gamma_b)$ where γ is the PAPR obtained using the best of Algorithms A1-A3 and γ_b is the PAPR obtained using QR factorization of $\mathbf{H}$, which corresponds to the choice $\mathbf{C} = \mathbf{I}$. As is evident from the plots and is generally true, algorithm A2 performs the best, but there are examples of channels matrices where the block algorithm A3 performs slightly better at low excess communication cost. Notice also that the variability is much smaller for algorithms A2 and A3, as compared to A1. This is true in general.

In order to give the reader a sense of the variability with different channel matrices, we plotted histograms of the relative PAPR, for a fixed excess communication cost for 1000 examples of randomly drawn $\mathbf{H}$. Entries in $\mathbf{H}$ were drawn iid $\mathcal{N}(0, 1)$. These results are in Fig. 6. It is interesting to note that for zero excess communication cost (leftmost pair, $d = 1$), small gains in PAPR are possible as compared to the direct QR factorization of $\mathbf{H}$. This result shows that in many cases, $\mathbf{C} \neq \mathbf{I}$ can result in a strict improvement in PAPR over $\mathbf{C} = \mathbf{I}$. The channel matrices were assume to be real-valued for this experiment.

In Fig. 7, we show simulation results obtained for the randomly selected channel matrix $H_8(P_e)$ displayed in App. D. This plot verifies correct operation of the distributed demodulator (curves labeled 'dfc') by comparing results to a hypothetical CN for the same precoder (curves labeled 'c'), which has access to unquantized RN observations. As can be seen the error probabilities are identical. In fact, the output of the centralized and distributed demodulator is identical. Curves labeled 'q' are for system S1, our baseline system. The output of the RN was quantized with a uniform quantizer having stepsize $1/d$, $d = 1$ and $d = 16$. We see that for $d = 1$, the error probability is high. For $d = 16$, the error probability is comparable to the new method, but the PAPR is significantly higher.

Finally, we investigate the effect that imprecise CSI has on system performance. Towards this end, we assume that a system has been designed based on channel matrix $\mathbf{H}$ but the actual channel is $\mathbf{H} + \mathbf{\Delta}$, where Δ is unknown to the transmitter, but is known to the receiver. More specifically, each entry in $\mathbf{\Delta}$ is $\pm\delta h_{ij}$, where h_{ij} is the ij entry of $\mathbf{H}$, and the $\pm$ sign chosen independently and with equal probability for each matrix entry. Two systems are investigated for real channels with $n = 4$, i.e the channel matrix is of size 4×4 and the results are presented in Figs. 8 for noise variance $\sigma^2 = 0$ and $\sigma^2 = 0.01$. The first system, whose performance is in the left hand column of each panel, is the rational-forcing precoder system in which the precoding matrix $\mathbf{S}$ is based on $\mathbf{H}$, and is chosen such that the receive lattice generator matrix $\mathbf{C} \in \mathcal{C}(3^{(3)})$. The second system, whose performance is shown in the right hand column of each panel, is the baseline system presented in Sec. VI-A, in which the precoder is based on channel matrix $\mathbf{H}$. Note that in both systems, the receive lattice generator matrix is a unit triangular matrix and $A = 7$. The RNs for both systems follow the same quantization strategy as before, i.e. the first RN uses a quantizer with step-size 1 and the ith RN uses quantizer step-size $1/3,\ i = 2, 3, 4$. In the CN, a zero-forcing filter first restores the triangular structure of the receiver lattice generator matrix. This is followed by a standard DFE decoder. The presented histograms of the error probability for each system are for 100 different channel realizations, in which the entries of $\mathbf{H}$ were drawn independently from a standard normal probability distribution, i.e. $h_{i,j} \sim \mathcal{N}(0, 1)$. For each channel realization, $100,000$ transmit and noise vectors were simulated. Three different values of δ, the relative inaccuracy, are presented in each figure, $\delta = 0$ (top row), $\delta = 0.01$

(middle row), corresponding to a 1% accuracy and $\delta = 0.05$ (bottom row) corresponding to a 5% accuracy, in the estimation of each element of $\mathbf{H}$. We see that the rational-forcing precoder is somewhat less sensitive to channel estimation errors as compared to the baseline system. Note that sensitivity to channel estimation errors was not a design consideration for either system.

VII. Summary, Conclusions and Future Work

We have considered the problem of communicating over a relay-assisted multiple-input multiple-output (MIMO) channel with additive noise, in which physically separated relays forward quantized information to a central decoder where the transmitted message is to be decoded. We assumed that channel state information is available in the transmitter. We have shown that a rational-forcing precoder matched to the quantizers in the RNs is useful for reducing the symbol error probability. This in turn has revealed a tradeoff between the decoder communication rate and the peak-average power ratio in the transmitter. We have presented several algorithms for constructing rational-forcing precoders. Our results have demonstrated that this approach can offer a designer a useful tool for trading PAPR with the excess communication cost in a distributed receiver.

An important problem for future work is that of interference management in multiple access settings. It is simple to serve multiple users using orthogonal physical layer resources (time or frequency), since the problem reduces to a point-to-point communication problem. When multiple users share the air-medium in a non-orthogonal manner, interference management is required. The techniques to be used will depend on the specific nature of the interferer, the amount of coordination that is allowed between base-stations and the relays. Just as this paper was based on a novel method for communication efficient computation of the Babai point, interference management awaits the development of novel communication efficient methods for implementing pre-coders across multiple base stations, and also communication efficient cooperative interference cancellation methodologies at the relays.

Acknowledgement

Thoughtful comments provided by the reviewers and the AE, which have helped to improve the presentation of the paper, are gratefully acknowledged.

VIII. FIGURES

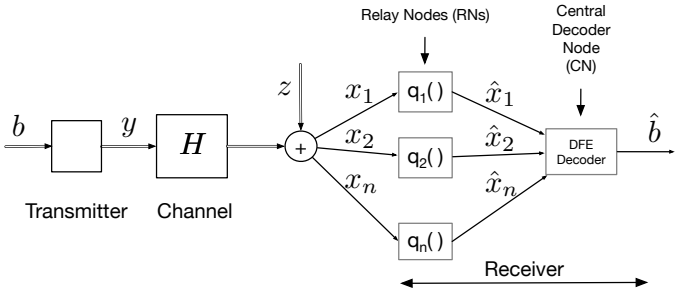

Fig. 1. System Diagram. $q_i(\cdot)$ represents the quantizer in the i-th RN.

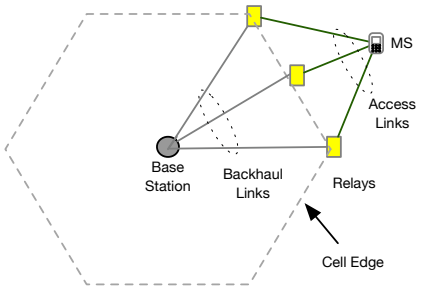

Fig. 2. Application scenario: relay-enhanced downlink for communicating information from the basestation to a mobile device (MS) with relays. The base-station to relay links are called backhaul links and the relay to-MS links are called access links. With reference to Fig. 1 we identify the transmitter with the Base Station and the MS with the CN. Access links are assumed to be noiseless.

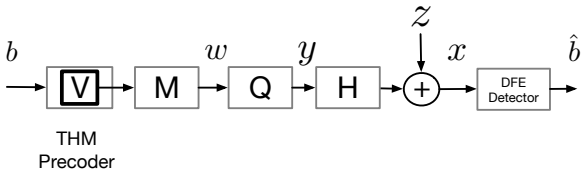

Fig. 3. Precoder and Receiver. The RN's, CN and connecting links are internal to the block marked DFE Detector.

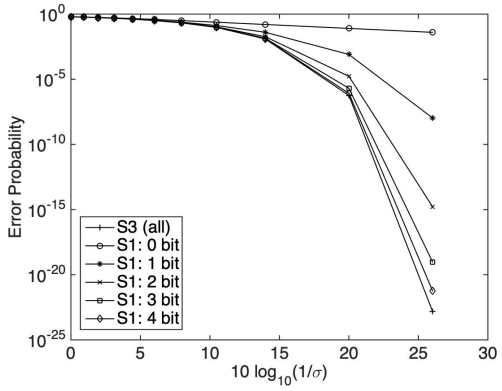

Fig. 4. Error probability as a function of noise variance σ for Strategies S1–S3. (S1:i bit): error probability for Strategy S1 with quantizer step size 2^{-i}. (S3:all): error probability for strategies S2 and S3 for all RN quantizer step sizes. Note that S2 and S3 use rational-forcing precoders.

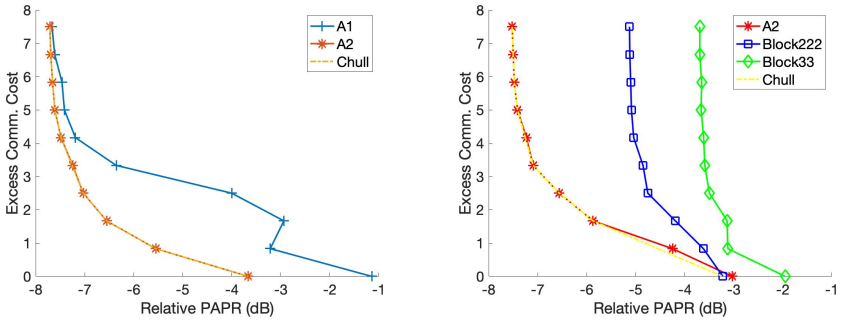

Fig. 5. Tradeoff between the excess communication cost, $R_{dec,ex}$ and relative PAPR for channel matrices $\mathbf{H}_6$ and $\mathbf{H}_6(Block)$ shown in App. D.

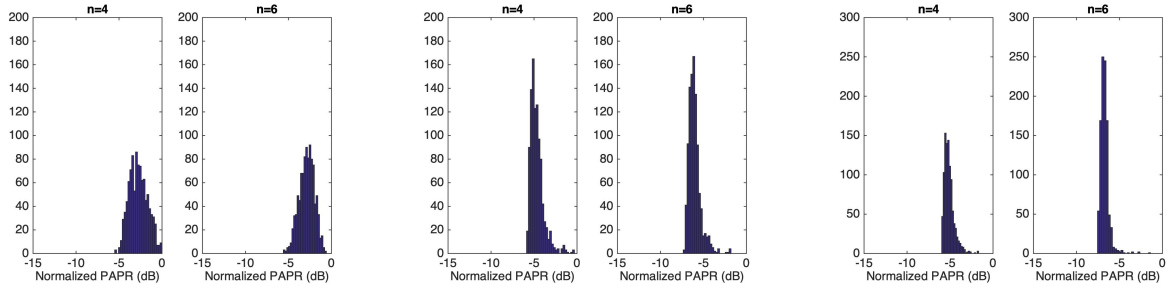

Fig. 6. Histogram of relative PAPR (dB) for $n = 4, 6$ based on 1000 trials. Left-right: each pair is for $\mathbf{C} \in \mathcal{C}(d^{(n-1)})$, $d = 1, 8, 32$.

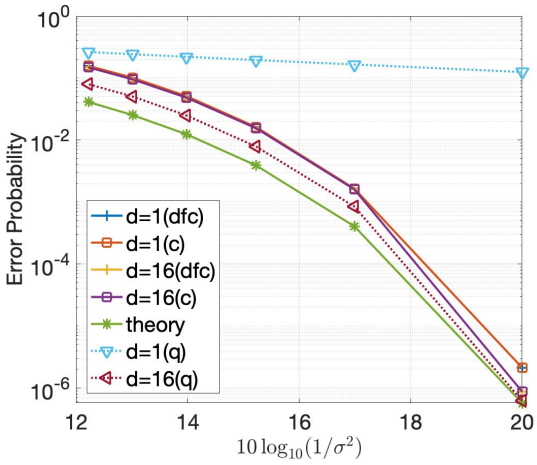

Fig. 7. Comparison of error probability for a fixed channel matrix for receive lattices, $\mathbf{C} \in \mathcal{C}(d^{(7)})$, $d = 1$ and 16. Curves labeled (c) are for a centrally decoded system, curves labeled (dfc) are for the rational-forcing precoder and curves labeled (q) are for the baseline system S1. For the rational-forcing precoder and S1, the quantizer in the i-th RN has step size $1/d$, $i = 2, 3, \ldots, n$ ($d = 1$ for $i = 1$). Curve labeled (theory) is from (15). Channel matrix is $\mathbf{H}_8(P_e)$ in the Appendix C.

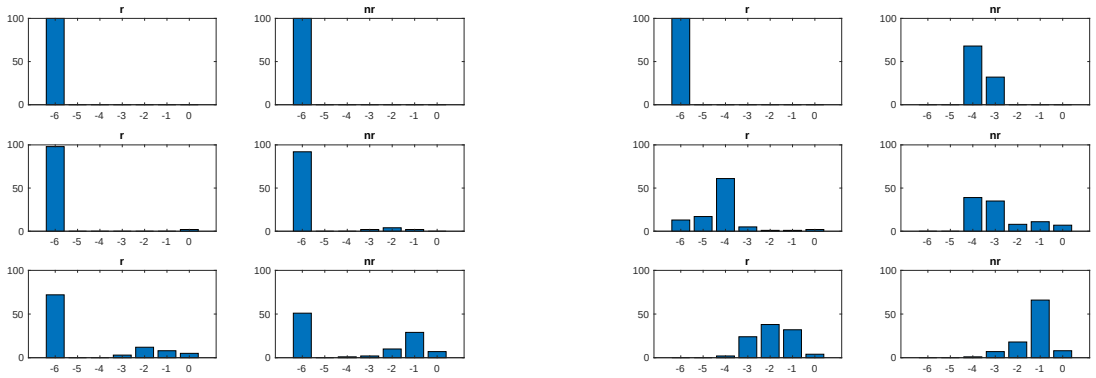

Fig. 8. Imperfect CSI in the transmitter. Histogram of error probability for 100 randomly drawn channels, $n = 4$. Noise variance: 0 (left panel), 0.01 (right panel). For each panel, top row : $\delta = 0$, middle row: $\delta = 0.01$ (1% accuracy), bottom row: $\delta = 0.05$. Left Column: rational-forcing precoder designed for $\mathbf{C} \in \mathcal{C}(3^{(3)})$, Right column, baseline precoder. For both systems, the quantizer step size in the first RN is 1 and in RNs $2-4$ is $1/3$. Horizontal axis: $\log_{10}(P_e)$.

APPENDIX A
THM PRECODER: DETAILS

Relevant implementation details for the THM-precoder are presented here. THM precoding [27], [14], was originally introduced for inter-symbol interference channels, and was more recently adapted to MIMO channels [8], [29]. Recall that the precoder $\mathbf{S}$ is such that $\mathbf{C} = \mathbf{Hs}$ is a unit lower triangular matrix and that $\mathbf{S} = \mathbf{QR}$ where $\mathbf{R}$ is upper triangular with real entries on the main diagonal and $\mathbf{Q}$ is unitary. Let $\mathbf{R} = \mathbf{MV}$, where $\mathbf{V}$ is unit upper triangular and $\mathbf{M}$ is a diagonal matrix with real entries. Let m_i be the *absolute value* of the ith diagonal entry of $\mathbf{M}$. From here on, the precoding for the real and imaginary parts separates, so we provide a description assuming real values. Pick real $A > 0$, such that $A/(2m_i)$ is not an integer for any i. Let $a_i = 2\lfloor A/(2m_i) - 1/2 \rfloor + 1$, $i = 1, 2, \ldots, n$.Let b_i, the ith component of the data vector $\mathbf{b}$, take values in the set $\{0, 1, \ldots, a_i - 1\}$. Thus the payload data rate is $R_{pay} = \lfloor \sum_{i=1}^{n} \log_2 a_i \rfloor$ bits/signaling interval. The THM-precoder computes

$$w_i = \underbrace{(b_i - a_i k_i)}_{b_i'} + \sum_{j=i+1}^{n} v_{i,j} \underbrace{(b_j - a_j k_j)}_{b_j'} \tag{29}$$

in the order $i = n, n-1, \ldots, 1$, where k_i is the unique integer for which w_i lies in the interval $[-a_i/2, a_i/2)$. Note that $b_i' = b_i - a_i k_i$ is an integer, $w_i \in [-A/(2m_i), A/(2m_i))$, $i = 1, 2, \ldots, n$ and $\mathbf{w} = \mathbf{Vb}'$. Note that in Fig. 3, and also later in the text, the THM-precoder implementation of $\mathbf{V}$ is denoted by $\boxed{\mathbf{V}}$.

Given w_i, $i = 1, 2, \ldots, n$, the information symbols, b_i' are recovered by

$$b_i' = \left\lceil w_i - \sum_{j=i+1}^{n} v_{i,j} b_j' \right\rceil \tag{30}$$

again in reverse order $i = n, n-1, \ldots, 1$, following which we obtain $b_i = b_i' \pmod{a_i}$.

The transmitted signal $\mathbf{y}$ is given by

$$\mathbf{y} = \mathbf{QMw} = \mathbf{QMVb}' = \mathbf{Sb}'. \tag{31}$$

Note that $\mathbf{Mw}$ lies in the hypercube $[-A/2, A/2]^n$ and assuming a uniform distribution on its support, the transmitted power is $\frac{1}{n} E[\|\mathbf{y}\|^2] = A^2/12$.

APPENDIX B
ERROR PROBABILITY AND QUANTIZATION: A GENERAL RESULT

We show that under certain conditions, quantization noise does not lead to an error floor. In our distributed receiver, the ith RN, sends a quantized version of its observation x_i to the CN. Assume that the CN has available a decoder $g : \mathbb{R}^n \to \mathbb{Z}^n$ (this is the decoder that would have been used if the RN observation was exactly available at the CN). It is intuitive that the quantization noise will 'add' to the channel noise, and thus we should expect

to see errors even when the channel noise is negligibly small. We show, in the following theorem that this is not the case, and that the error probability *is not* limited by the quantization process, provided the quantizer is suitably fine.

Assume that each observation x_i is quantized by the RN using a uniform quantizer with infinite support, and the bin size of each quantizer is Δ. The bin index is communicated to the CN using entropy coding, say with a Huffman code. We now study the behavior of the error probability $P_e = Prob[\hat{\mathbf{b}} \neq \mathbf{b}]$, as the noise variance $\sigma^2 \to 0$. Denote the inverse image of information vector $\mathbf{b}$ under the action of the decoder g by

$$g^{-1}(\mathbf{b}) = \{\mathbf{x} \ : \ g(\mathbf{x}) = \mathbf{b}\} \subset \mathbb{R}^n.$$

Given a set $A \subset \mathbb{R}^n$, we use the notation A^{o} to denote its *interior* and vol(A) to denote its volume.

Theorem 1. *Suppose that the decoder has the property that* $\mathbf{b} \in g^{-1}(\mathbf{b})^{\mathrm{o}}$ *for all* $\mathbf{b} \in \mathbb{Z}^n$ *and that vol*$(g^{-1}(\mathbf{b})) > v_0 > 0$*, for some positive constant* v_0*. Then there is a quantizer step size* Δ*, suitably small, such that* $\lim_{\sigma \to 0} P_e = 0$*.*

Proof: There is a $\gamma > 0$ such that for any $\mathbf{b} \in \mathbb{Z}^n$, the hypercube with vertices $b_i \pm \gamma$, $i = 1, 2, \ldots, n$ lies in $g^{-1}(\mathbf{b})^{\mathrm{o}}$. Choose $\Delta = \gamma/2$. The uniform quantizer with bin size Δ partitions $\mathbb{R}^n$ into cells. Mark with a $*$, every quantizer cell which contains an information vector $\mathbf{b} \in \mathbb{Z}^n$. The probability that the quantized channel output corresponding to information vector $\mathbf{b}$ lies in the $*$-cell corresponding to $\mathbf{b}$ converges to 1 as $\sigma \to 0$. Hence for any quantizer step size smaller that $\gamma/2$, the CN will recover $\mathbf{b}$ without error in the limit $\sigma \to 0$. ■

APPENDIX C
OPTIMALITY OF UNIFORM QUANTIZATION IN THE RNS

Earlier we had shown that if the RN's use quantizers with step sizes $s_1 = 1$, $1/s_i$, $i = 2, \ldots, n$, s_i positive integers, then designing a precoder whose elements in the ith row are expressible as rationals with denominator s_i results in an absence of an interference term, as seen in (14). Here we use results from the area of *distributed function computation* to show the dual result, namely, if $\mathbf{C}$ is a unit triangular matrix then the decoder communication rate is minimized by using an appropriately chosen uniform quantizer. For this to be true we assume that x_i, $i = 1, 2, \ldots, n$ are independent. We will assume here that the lattice generator matrix $\mathbf{C}$ is a rational unit lower triangular matrix.

The function that maps $\mathbf{x}$ to the the ith component of the Babai point is denoted $f_b^{(i)}$, and we define $f_b = (f_b^{(1)}, f_b^{(2)}, \ldots, f_b^{(n)})$. Note that f_b is a composition of the maps f and q_i defined in (1), specifically $\hat{b} = f_b(\mathbf{x}) = f(q_1(x_1), q_2(x_2), \ldots, q_n(x_n))$. Thus $\hat{b}_m = f_b^{(m)}(\mathbf{x})$ in (7). It is shown in [22], [9], the sum rate for computing f_b, i.e. the minimum number of bits that the RNs need to send to the CN in order that the CN compute f_b correctly, must satisfy $R_{sum} \geq \sum_{i=1}^n H_{G(i)}(x_i|\mathbf{x}_{\text{-}i})$, where $H_{G(i)}(x_i|\mathbf{x}_{\text{-}i})$ is the graph-entropy of the characteristic graph $G(i)$ of $f_b^{(i)}$, conditioned on $(x_i, i = 1, 2, \ldots, i-1, i+1, \ldots, n)$. The structure of the characteristic graphs $G(i)$ will be de-

scribed in more detail in the next paragraph. For simplicity, we use the notation $\mathbf{x}_{\text{-}i} = (x_1, \ldots, x_{i-1}, x_{i+1}, \ldots, x_n)$, i.e. the $(n-1)$-dim vector obtained by excluding x_i from $\mathbf{x}$. Additionally, given an $(n-1)$ dimensional vector $\mathbf{y}$ and a scalar x, let $(x \rightarrow_i y)$ be the vector obtained by inserting x into $\mathbf{y}$ in the ith position. Thus $\mathbf{x} = (x_i \rightarrow_i \mathbf{x}_{\text{-}i})$.

We first obtain the characteristic graphs $G(i)$ for $f_b^{(i)}$ and show that their maximal independent sets are intervals. From the definition [22], $G(i)$ is a graph whose nodes are the support set for the random variable x_i, (which is $\mathbb{R}$) and (x, x') is an edge of $G(i)$ if there is an $(n-1)$-dim vector $\mathbf{y}$ for which $f_b^{(i)}((x \rightarrow_i \mathbf{y})) \neq f_b^{(i)}((x' \rightarrow_i \mathbf{y}))$.

Let us first consider $G(1)$. Observe that since $b_1 = [x_1]$, x_1 is *disconnected* from x_1' in $G(1)$ if and only if both lie in the interval $[(l-1/2), (l+1/2))$ for some integer l, or equivalently (x_1, x_1') is an edge if and only if $x_1 \in [(l-1/2), (l+1/2))$ and $x_n' \in [(m-1/2), (m+1/2))$ for $m \neq l$. Thus, the maximal independent sets of the graph $G(1)$ are the disjoint intervals $[(z-1/2), (z+1/2))$, $z \in \mathbb{Z}$ and can be indexed by an integer valued random variable Z_1. Further, these intervals partition $\mathbb{R}$.

Now consider the graph $G(m)$, $m > 1$ and its maximal independent sets. Assume that in (7) the term $\sum_{l=1}^{m-1} c_{m,l} b_l$ is an integer multiple of r/s, where r and s are relatively prime. In order to construct the characteristic graph $G(m)$, we must find values of x such that $[x - kr/s] = j$, for every $k \in \mathbb{Z}$. Here we will use the following definition for the fractional part: $\{x\} = x - \lfloor x \rfloor$. Since $[x - kr/s] = [x - \{kr/s\}] - \lfloor kr/s \rfloor$ and kr/s is known at the decoder it suffices to find values of x for which $[x - \{kr/s\}] = j$ for all $k \in \mathbb{Z}$. It follows that x must satisfy

$$j - 1/2 + l/s \leq x < j + 1/2$$

for all l such that $-1/2 + l/s < 1/2$. From here it follows that

$$j + 1/2 - 1/s \leq x < j + 1/2$$

which in turn gives us

$$sj + s/2 - 1 \leq sx < sj + s/2.$$

Thus for s even (odd), $[x - \{kr/s\}]$ is constant independent of k if and only if $\lfloor sx \rfloor$ ($[sx]$) is a constant. It follows that (x_m, x_m') is an edge in $G(m)$ if and only if $\lfloor sx_m \rfloor \neq \lfloor sx_m' \rfloor$ for s even and $[sx_m] \neq [sx_m']$ for s odd. These disjoint intervals are the maximally independent sets of $G(m)$ and they partition $\mathbb{R}$.

We have thus shown that the maximally independent sets of each of the graphs $G(i)$, $i = 1, 2, \ldots, n$ are disjoint intervals that partition $\mathbb{R}$.

Let $\mathcal{Z}_i$ denote the collection of maximally independent sets of $G(i)$ and let z_i be a random variable which takes values in $\mathcal{Z}_i$. From [22] we know that $H_{G(i)}(x_i|x_{\text{-}i})$, the conditional graph-entropy of $G(i)$ is by definition the minimum conditional mutual information $I(z_i; x_i|x_{\text{-}i})$, where the minimum is over all conditional distributions $P(z_i|x_i, x_{\text{-}i})$ which satisfy

1) the Markov condition $P(z_i|x_i, x_{\text{-}i}) = P(z_i|x_i)$,
2) $\sum_{z\in\mathcal{Z}_i \,:\, x_i\in z} P(z|x_i) = 1$.
3) $P(z|x_i) = 0$, if x_i is not in the interval indexed by z.

Since z_i is uniquely determined by x_i it follows that $H(z_i|x_i) = 0$ and hence $H_{G(i)}(x_i|x_{\text{-}i}) = \min I(x_i; z_i|x_{\text{-}i}) = H(z_i|x_{\text{-}i}) = H(z_i)$. Thus the minimum rate for computing the Babai point is bounded below by $\sum_{i=1}^{n} H(z_i)$, which is precisely equal to $nR_{dec,ex}/(n-1)$ from (17).

APPENDIX D
MATRICES

$$\mathbf{H}_1 = \begin{pmatrix} -0.5500 & -0.8528 & -0.2253 & 0.7411 \\ 0.8270 & 0.7026 & 1.3365 & 0.0944 \\ 0.4247 & -0.5069 & 1.1926 & 0.5349 \\ 1.8389 & 1.2790 & 0.7321 & 1.2229 \end{pmatrix},\ \mathbf{C}_1 = \begin{pmatrix} 1 & 0 & 0 & 0 \\ -1 & 1 & 0 & 0 \\ 0 & 2 & 1 & 0 \\ -3 & 3 & 3 & 1 \end{pmatrix}.$$

$$Re(\mathbf{H}_6) = \begin{pmatrix} -0.52708 & -0.02289 & -0.21550 & 0.67585 & -0.38096 & 0.08709 \\ 0.40223 & 0.27959 & -0.44671 & 0.46192 & -0.36614 & 0.76415 \\ 0.20768 & 0.19238 & 0.56964 & 0.30253 & 0.77867 & 0.08066 \\ 0.15626 & -0.10246 & -0.57722 & -0.18397 & 0.42524 & -0.81392 \\ -0.50247 & -0.10582 & -0.01805 & 0.42927 & -0.83168 & 0.11605 \\ 0.35644 & 0.32059 & -0.07412 & 0.00940 & -0.34596 & -0.43395 \end{pmatrix}$$

$$Im(\mathbf{H}_6) = \begin{pmatrix} -0.37826 & 0.57284 & 0.42027 & 0.03254 & -0.38014 & -0.04484 \\ -0.38028 & 0.32338 & 0.36868 & 0.15508 & -0.10933 & -0.32468 \\ 0.61721 & -0.50284 & 0.64718 & 0.65885 & -0.83420 & 0.71394 \\ -0.07854 & -0.24704 & -0.38027 & 0.46033 & -0.24229 & -0.51102 \\ -0.37907 & 0.52474 & -0.22465 & -0.27828 & -0.81634 & 0.54388 \\ -0.21661 & 0.07476 & 0.12050 & 0.09971 & 0.68824 & 0.65266 \end{pmatrix}$$

$$Re(\mathbf{H}_6(block)) = \begin{pmatrix} 1.46153 & -0.92029 & -0.07365 & -1.00508 & 0.34118 & 0.16772 \\ 0.52876 & -0.13722 & -0.01545 & -0.05679 & 1.22040 & 0.13101 \\ 0.36383 & -0.29326 & 0.67498 & 0.45669 & -0.67056 & 0.26865 \\ -0.49097 & 0.32702 & 0.26575 & -0.37915 & 0.48261 & -0.57415 \\ -0.12887 & 0.20168 & 0.03722 & 0.24747 & 0.16994 & 0.69213 \\ 0.55728 & 0.21577 & 0.18936 & -0.00361 & -0.68836 & -0.36150 \end{pmatrix}$$

$$Im(\mathbf{H}_6(block)) = \begin{pmatrix} 0.14573 & 0.16081 & -0.21373 & 0.82726 & 0.05970 & -0.29838 \\ -0.00611 & -0.98424 & -0.40453 & -0.44198 & -0.34289 & -0.73872 \\ 0.26219 & -0.09613 & 0.15921 & -0.59757 & 0.34099 & -0.87118 \\ -0.00603 & -0.04943 & -0.30453 & 0.03197 & 0.49478 & -0.28369 \\ 0.16894 & -0.00265 & 0.37323 & 0.03180 & 0.55557 & -0.09078 \\ 0.46615 & -0.23594 & 0.01049 & -0.84908 & 0.55676 & 0.63640 \end{pmatrix}$$

$$\mathbf{H}_8(P_e) = \begin{pmatrix} -0.65632 & -0.09014 & 0.00161 & -0.73252 & 0.63072 & -0.25749 & -0.60295 & 0.44435 \\ -0.08795 & 1.00030 & 1.13019 & -0.74737 & -0.83234 & 0.74225 & -0.02748 & 1.56517 \\ -1.16431 & -0.61602 & 1.18848 & -1.12751 & 0.53695 & -0.18663 & 1.09393 & -0.22883 \\ -0.81324 & 0.34531 & -2.12999 & 0.64501 & 0.02904 & -0.21989 & 0.75009 & -0.09109 \\ -1.54177 & 1.39277 & 0.93949 & -0.05664 & 0.11375 & -0.10148 & -0.87527 & 0.10403 \\ -0.92881 & -2.61595 & -2.01614 & -0.04005 & -0.40333 & 0.47592 & 1.39063 & -1.93956 \\ -0.30483 & 0.14573 & -0.62909 & 1.93598 & 0.05903 & -1.23895 & -0.05763 & 2.07281 \\ 1.35382 & -0.57728 & 2.51142 & 0.68710 & -0.36337 & -1.20280 & -2.08635 & 0.83606 \end{pmatrix}$$

REFERENCES

[1] L. Babai. “On Lovász lattice reduction and the nearest lattice point problem”. *Combinatorica*, vol. 6, no. 1, pp. 1-13, Mar. 1986.

[2] R. W. Bauml, R. F. H. Fischer, and J. B. Huber. ”Reducing the peak-to-average power ratio of multicarrier modulation by selected mapping.” Electronics letters, vol. 32, no. 22, pp. 2056-2057, 1996.

[3] M. F. Bollauf, V. A. Vaishampayan, and Sueli I. R. Costa. “On the communication cost of determining an approximate nearest lattice point”, in Proc., IEEE Intl. Symposium Information Theory, Aachen, Germany, pp. 1838-1842, June 2017.

[4] M. F. Bollauf, V. A. Vaishampayan, and Sueli I. R. Costa. “Communication and error probability for distributed computation of the Babai point”, in preparation.

[5] G. Caire and S. Shamai. ”On the achievable throughput of a multiantenna Gaussian broadcast channel,” IEEE Transactions on Information Theory, vol. 49, no. 7, pp. 1691-1706, June 2003.

[6] X.-W. Chang, J. Wen, and X. Xie. ”Effects of the LLL reduction on the success probability of the Babai point and on the complexity of sphere decoding.” IEEE Transactions on Information Theory, vol. 59, no. 8, pp. 4915-4926, Aug. 2013 .

[7] L. J. Cimini, and N. R. Sollenberger. ”Peak-to-average power ratio reduction of an OFDM signal using partial transmit sequences.” IEEE Communications Letters, vol. 4, no. 3, pp. 86-88, March 2000.

[8] I. B. Collings and I. V. L. Clarkson. ”A low-complexity lattice-based low-PAR transmission scheme for DSL channels.” IEEE Transactions on Communications, vol. 52, no. 5, pp. 755-764, May 2004.

[9] A. El Gamal and Y. H. Kim, Network Information Theory. Cambridge University Press, 2011.

[10] R. F. Fischer and C. A. Windpassinger, “Improved MIMO precoding for decentralized receivers resembling concepts from lattice reduction,” In Proc. IEEE Global Telecommunications Conference, vol. 4, pp. 1852-1856, Dec. 2003.

[11] R. F. H. Fischer and M. Hoch, ”Peak-to-average power ratio reduction in MIMO OFDM,” In Proc. 2007 IEEE International Conference on Communications, pp. 762-767, June 2007.

[12] G. J. Foschini, G. D. Golden, R. A. Valenzuela and P. W. Wolniansky, “Simplified processing for high spectral efficiency wireless communication employing multi-element arrays,” IEEE Journal on Selected areas in communications, vol. 17, No. 11, pp.1841-1852.

[13] G. H. Golub and C. F. Van Loan, *Matrix Computations*. Johns Hopkins University Press, 1996.

[14] H. Harashima and H. Miyakawa, “Matched-transmission technique for channels with intersymbol interference,” IEEE Trans- actions on Communications, vol. 20, no. 4, pp. 774–780, August 1972.

[15] R. A. Horn and C. R. Johnson. *Matrix analysis*. Cambridge University Press, 1985.

[16] M. Joham, W. Utschick and J. A. Nossek, ”Linear transmit processing in MIMO communications systems,” IEEE Transactions on Signal Processing, vol. 53, no. 8, pp. 2700-2712, Aug. 2005.

[17] A. E. Jones, T. A. Wilkinson, and S. K. Barton. “Block coding scheme for reduction of peak to mean envelope power ratio of multicarrier transmission schemes.” Electronics Letters, vol. 30, no. 25, pp. 2098-2099, Dec. 1994.

[18] A. K. Lenstra, H. W. Lenstra ,and L. Lovász, “Factoring polynomials with rational coefficients,” Mathematische Annalen, vol. 261, no. 4, pp. 515-534, 1982.

[19] V. Loscri, Y. Hong and E. Viterbo. ”RQ precoding for the cooperative broadcast channel,” In Proc. 2009 IEEE Information Theory Workshop, pp. 26-30, Oct. 2009.

[20] S. Lyu and C. Ling, “Boosted KZ and LLL Algorithms,” IEEE Trans. Signal Processing, vol. 65, No. 18, pp. 4784-4796, 2017. Matlab Code Source: https://codeocean.com/capsule/8604047/tree/v1

[21] M. A. Maddah-Ali, M. A. Sadrabadi, and A. K. Khandani. ”Broadcast in MIMO systems based on a generalized QR decomposition: Signaling and performance analysis.” IEEE Transactions on Information Theory, vol. 54, no. 3, pp. 1124-1138, Feb. 2008.

[22] A. Orlitsky and J. R. Roche, “Coding for Computing,” IEEE Transactions on Information Theory, vol. 47, no. 3, pp. 903–917, Mar. 2001.

[23] O’Neill, Rorie, and Luis B. Lopes. “Performance of amplitude limited multitone signals,” In Proceedings of IEEE Vehicular Technology Conference (VTC), pp. 1675-1679, 1994.

[24] C. Saha, M. Afshang and H. S. Dhillon, ”Bandwidth Partitioning and Downlink Analysis in Millimeter Wave Integrated Access and Backhaul for 5G,” in IEEE Transactions on Wireless Communications, vol. 17, no. 12, pp. 8195-8210, Dec. 2018, doi: 10.1109/TWC.2018.2874655.

[25] G. W. Stewart, “Perturbation bounds for the QR factorization of a matrix,” SIAM Journal on Numerical Analysis, vol. 14, No. 3, pp. 509-518, June 1977.

[26] E. Telatar, ”Capacity of multi-antenna Gaussian channels,” European Trans. on Telecommunications, vol. 10, No. 6, pp.585-595, Nov. 1999.

[27] M. Tomlinson, “New automatic equaliser employing modulo arithmetic,” Electronics Letters, vol. 7, no. 5, pp. 138–139, March 1971.

[28] H. Utatsu, K. Osawa, J. Mashino, S. Suyama and H. Otsuka, ”Throughput Performance of Relay Backhaul Enhancement Using 3D Beamforming,” 2019 International Conference on Information Networking (ICOIN), Kuala Lumpur, Malaysia, 2019, pp. 120-124, doi: 10.1109/ICOIN.2019.8718197.

[29] C. Windpassinger, Christoph, R. F. H Fischer, T. Vencel, and J. B. Huber. ”Precoding in multiantenna and multiuser communications,” IEEE Transactions on Wireless Communications, vol. 3, no. 4, pp. 1305-1316, July 2004.

[30] A. C. Yao. “Some Complexity Questions Related to Distributive Computing(Preliminary Report)” in *Proc. of the Eleventh Annual ACM Symposium on Theory of Computing*, 1979, pp. 209-213.

[31] H. Yao and G. W. Wornell. ”Lattice-reduction-aided detectors for MIMO communication systems,” In Proc. Global Telecommunications Conference, GLOBECOM’02, vol. 1, pp. 424-428, Nov. 2002.